Probing the Binding of Indolactam-V to Protein Kinase C through Site-Directed Mutagenesis and Computational Docking Simulations

Shaomeng Wang,*,† Ming Liu,† Nancy E. Lewin,‡ Patricia S. Lorenzo,‡ Dipak Bhattacharrya,‡ Lixin Qiao,† Alan P. Kozikowski,† and Peter M. Blumberg*,‡

Drug Discovery Program, Georgetown Institute for Cognitive and Computational Sciences, Research Building, Room EP07, Georgetown University Medical Center, 3970 Reservoir Road, Washington, D.C. 20007, and Laboratory of Cellular Carcinogenesis and Tumor Promotion, Division of Basic Sciences, National Cancer Institute, National Institutes of Health, Bethesda, Maryland 20892

Received March 18, 1999

Protein kinase C (PKC) comprises a family of ubiquitous enzymes transducing signals by the lipophilic second messenger *sn*-1,2-diacylglycerol (DAG). Teleocidin and its structurally simpler congener indolactam-V (ILV) bind to PKC with high affinity. In this paper, we report our computational docking studies on ILV binding to PKC using an automatic docking computer program, MCDOCK. In addition, we used site-directed mutagenesis to assess the quantitative contribution of crucial residues around the binding site of PKC to the binding affinity of ILV to PKC. On the basis of the docking studies, ILV binds to PKC in its cis-twist conformation and forms a number of optimal hydrogen bond interactions. In addition, the hydrophobic groups in ILV form "specific" hydrophobic interactions with side chains of a number of conserved hydrophobic residues in PKC. The predicted binding mode for ILV is entirely consistent with known structure−activity relationships and with our mutational analysis. Our mutational analysis establishes the quantitative contributions of a number of conserved residues to the binding of PKC to ILV. Taken together, our computational docking simulations and analysis by site-directed mutagenesis provide a clear understanding of the interaction between ILV and PKC and the structural basis for design of novel, high-affinity, and isozyme-selective PKC ligands.

Introduction

Protein kinase C (PKC) comprises a family of ubiquitous signal-transducing enzymes, which play a key role in the regulation of cell growth, differentiation, apoptosis, ion channels, neurotransmitter release, and neuronal plasticity.[1−4] All the PKC isozymes discovered to date, with the exception of PKCζ and PKCλ, are activated under physiological conditions through the binding to the cofactors phospholipid and the two second messengers Ca^{2+} and diacylglycerol (DAG) (Ca^{2+} is required only for the Ca^{2+}-dependent PKC isozymes).[1−5] PKC is the primary receptor for the powerful tumor-promoting agents phorbol esters, ingenol esters, mezerein, and aplysiatoxin and for teleocidins and their structurally simpler congener, indolactam (ILV).[6,7] These PKC ligands serve as structural mimetics of DAG[6,7] and bind to either of the two cysteine-rich domains (C1a, C1b) in PKC with nanomolar binding affinity.[8,9]

The precise interaction mechanism between PKC and its ligands has attracted much attention because of its critical importance to the understanding of the activation of PKC and of tumor promotion.[6−10] A detailed 3D picture of the interactions between PKC and its ligands would also be invaluable for the rational design of novel PKC modulators. Since phorbol esters, teleocidins, ILV, and other high-affinity PKC ligands compete with DAG for binding to PKC, it has been hypothesized that these structurally diverse ligands may share common, 3D structural binding features, or a so-called "pharmacophore", that acts as the structural basis for the binding of these ligands to PKC. In the past, in the absence of knowledge regarding the 3D PKC receptor structure, molecular modeling studies have been conducted by several groups to elucidate the 3D pharmacophore shared by these PKC ligands, based upon the 3D structures of ligands and structure−activity relationships (SARs).[12] A number of pharmacophore models have been proposed,[12] and these models were used to help in the design of potent PKC ligands[19,22] and the discovery of novel PKC ligands through a 3D database pharmacophore search approach.[23]

Each of the PKC isozymes contains a regulatory domain and a catalytic domain. Within their regulatory domains, both classical (α, β, and γ) and novel (δ, ϵ, η, and θ) PKC isozymes contain two cysteine-rich domains (C1a, C1b), each of which can bind to phorbol esters with high affinity.[5] Recently, the crystal structures of PKCδ C1b (residues 231−280 in PKCδ; renumbered as 1−50 in this paper) alone and in complex with phorbol-13-acetate were solved by X-ray crystallography.[11] The X-ray complex structure revealed for the first time precisely where and how phorbol ester binds to PKC. It showed that phorbol-13-acetate binds between residues 8−12 and 20−27; the binding is governed by a number of strong hydrogen bonds. The orientations of these main chain groups in PKC are controlled by a set of highly conserved residues. These two phorbol ester

* To whom correspondence and requests of reprints should be addressed. E-mail: wangs@giccs.georgetown.edu (S.W.) or blumberp@dc37a.nci.nih.gov (P.M.B.).
† Georgetown University Medical Center.
‡ NIH.

10.1021/jm990129n CCC: $18.00
Published on Web 08/21/1999

binding segments (8−12 and 20−27) are well-ordered in the crystal in the presence and absence of phorbol ester.[11] The comparison of the X-ray structures in the absence and the presence of phorbol ester showed that the phorbol binding site does not undergo any significant conformational change upon the binding of the phorbol ester.[11] The crystal structure of these two phorbol ester binding segments is equally rigid regardless of phorbol binding. Hence, the X-ray structure of PKCδ C1b provides us with a solid structural basis and an excellent opportunity to elucidate the binding of other high-affinity ligands to PKC.

A previously commonly accepted pharmacophore model for phorbol ester binding to PKC, proposed by Rando and Kishi,[16,17] consists of the hydroxyl groups at C9 and C20 and the carbonyl group at C3. The pharmacophore model was proposed based upon the nice overlap between the 3D structures of phorbol esters, the endogenous ligand DAG, and other classes of PKC ligands.[16,17] The X-ray structure of PKC in complex with phorbol-13-acetate[11] showed that the carbonyl group at C3 and the hydroxyl group at C20 of phorbol-13-acetate form three strong hydrogen bonds with PKC, in agreement with the pharmacophore model.[16,17] The hydroxyl group at C9, surprisingly, does not have apparent hydrophophilic/hydrogen bond interactions with PKC but forms an intramolecular hydrogen bond with the ester group at C13 of phorbol ester. In addition, the hydroxyl group at C4, functioning as a hydrogen bond donor, forms a strong hydrogen bond with the backbone carbonyl group of Gly 23 in PKC, suggesting its important role in phorbol ester binding to PKC, which was not implicated in the previous pharmacophore model.[16−18] The discrepancies between the previously proposed pharmacophore model[16−18] and the pharmacophore revealed by the X-ray structure[11] has a number of implications. First, it suggested that the commonly accepted pharmacophore model for phorbol esters and other PKC ligands is not entirely correct. Second, the concept that all PKC ligands should share a common 3D pharmacophore is not valid and should be reevaluated.

Teleocidin and its structurally simpler congener, ILV, exemplify a class of high-affinity PKC ligands, and their SARs have been investigated in a number of laboratories.[24−28] This class of high-affinity PKC ligands is synthetically more accessible than the phorbol esters, and therefore they may represent excellent lead compounds for the design of novel, non-tumor-promoting, and isozyme-selective PKC modulators. Previous modeling attempts have had difficulties in identifying what constitutes the pharmacophore in this class of compounds, in part due to the conformational flexibility of teleocidin and ILV.[12,14,16] Both ILV and teleocidin exist in an equilibrium of two conformational states in solution, namely cis-twist and trans-sofa forms.[24] Although the trans-sofa conformation was thought to be the biologically active conformation,[14] recent experimental evidence indicated that the cis-twist conformation is the biologically active one.[25,28]

Undoubtedly, a detailed 3D picture of the interactions between teleocidin, ILV, and PKC would provide additional insight into the mechanism of PKC activation and the structural basis for the design of novel PKC modulators based upon this class of compounds. It will also provide us an opportunity to examine the validity of previously proposed, ligand-based pharmacophore models for PKC ligands. In the present study, we report our molecular modeling and site-directed mutational analysis of the binding of ILV to PKC.

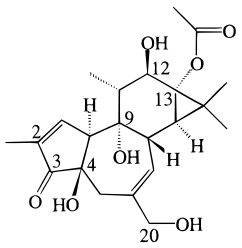

Phorbol-13-acetate

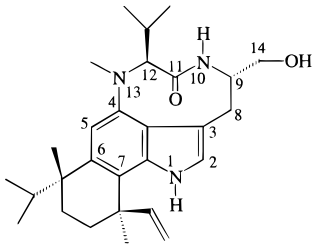

Teleocidin B-4

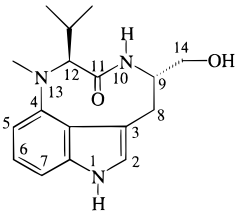

Indolactam-V (ILV)

Methods and Materials

1. Computational Studies. (a) Docking simulations: Computational docking simulations were carried out using the MCDOCK program recently developed in our laboratory.[29] Briefly, MCDOCK employs a nonconventional Monte Carlo (MC) simulation technique and carries out the docking operation fully automatically. The current version of the MCDOCK program (version 1.0) takes account of the full flexibility of ligands. The scoring function used in MCDOCK is the sum of the interaction energy between the drug molecule and its receptor and the conformational energy of the drug molecule. The structural input data for the MCDOCK program are the 3D coordinates of the receptor (enzyme) and the drug molecule. MCDOCK includes three stages of calculations: geometry-based MC docking, energy-based MC docking, and final energy minimization.

The X-ray coordinates of PKCδ C1b in complex with phorbol-13-acetate[11] were used as the receptor structure in our docking studies. The 3D structure of ILV was built starting from the X-ray structure of teleocidin[30] using the QUANTA program.[31] The structure of ILV was first minimized using the CHARMM program and then reminimized using the Gaussian 92 program[32] with the 3-21G* basis set. Mulliken atomic charges for ILV were calculated using the Gaussian 92 program[32] with the 6-31G* basis set and were used in the MCDOCK docking simulations and to build the residue topology file (RTF) for ILV in subsequent minimization and molecular dynamics simulations.

(b) Further refinement of binding mode: With the MCDOCK-predicted binding modes, further refinement was carried out using the CHARMM program[33] (version 24), with the version 22 MSI parameter set, running on an SGI indigo2/R10000 workstation. An adopted-basis Newton Raphson algorithm, implemented in the CHARMM program, was used in the energy minimizations. Energy was minimized for 10 000 steps for the complex structure, or until convergence, defined as an energy gradient $\leq$ 0.001 kcal/mol^{-1} Å^{-1}. A constant dielectric was used and set to 1. The nonbonded cutoff distance was set to 14.0 Å. A shifted smoothing function was used for the van der Waals interaction and a switch function for the electrostatic energy calculation. The cutoff distance parameters used in the smoothing functions were as follows: CTOFNB = 12.0 Å; CTONNB = 8.0 Å.

Molecular dynamics simulations were employed to further refine the structure of ILV in complex with PKC. The complex structure was solvated with 538 TIP3P water molecules.[34] The system was heated to 300 K in a period of 5 ps and equilibrated for 20 ps at 300 K. Finally, 100-ps or longer constant temperature simulations were performed at 300 K with a step size of 0.001 ps. Trajectories were recorded every 0.1 ps during the simulations and analyzed. A shake algorithm was used to constrain bonds to hydrogen.[35]

(c) Analysis of the binding mode: Hydrogen bonds are crucial for the interactions between PKC ligands and PKC, as evident from the X-ray structure of phorbol-13-acetate and PKC. Hydrogen bonds involve atoms AA, A, H, and D (acceptor antecedent, acceptor, hydrogen, and donor heavy atom). The strength of a hydrogen bond not only depends on the nature of the hydrogen bond donor and acceptor but also depends on at least three geometrical parameters: the distance between the acceptor and donor (r_{AD}) and two angles (θ_{A-H-D} and θ_{AA-A-H}). To provide a quantitative analysis of the strength of hydrogen bonds, the following equation was used in the calculations of hydrogen bond energy:

$$E_{HB} = (Ar_{DA}^{-6} - Br_{DA}^{-4}) \cos^2(\theta_{D-H-A}) \cos(\theta_{H-A-AA} - (\theta_{H-A-AA})^{optimal}) \quad (1)$$

where the E_{HB} is the hydrogen bond energy for a particular hydrogen bond and A and B are constants and depend on the nature of the hydrogen bond donor and acceptor groups. In our hydrogen bond evaluations, since we are more concerned if a hydrogen bond was optimal, we have assumed that each of these hydrogen bonds formed between the ligand and the receptor assumed an optimal value of −4 kcal/mol. The optimal hydrogen bond distance between the donor and acceptor atoms is around 2.8−3.0 Å. We chose 3.0 Å as the optimal distance for all the hydrogen bonds in our calculations. It has been shown that the optimal value for θ_{D-H-A} is around 160−180°, and for simplicity, we assumed the optimal value of 180°. It has been shown that the optimal value for θ_{H-A-AA} is around 120°; therefore, the optimal value of $(\theta_{H-A-AA})^{optimal}$ was set to be 120° in our evaluations. Under these conditions, A and B assumed the values of 5832 and 972, respectively.

In addition to hydrogen bonds, we and others have shown that hydrophobic interactions play a crucial role in the binding of PKC ligands to PKC.[28,36] In the current study, we have carried out a quantitative analysis of the hydrophobic interactions between ILV and PKC using the HINT program[37−39] running under the Chem-X program,[40] running on a Silicon Graphics Indigo2/R10000 with IRIS 6.2. The log P value for the ligand was calculated using the "calculate" option, and the log P value for the protein was calculated using the "dictionary" option in the HINT program. The intermolecular hydrophobic interaction map and table were generated for the trajectories recorded at the end of each 10-ps simulation period during the 100-ps CHARMM molecular dynamics simulations. The HINT values were calculated using the following equation:

$$b_{ij} = s_i a_i s_j a_j R_{ij} \langle \text{summed for all } i, j \rangle$$

where b_{ij} is a microinteraction constant representing the attraction/interaction between atoms i and j, s_i and s_j are the solvent-accessible surface areas for i and j, respectively, a_i and a_j are the hydrophobic atom constants for i and j, respectively, and R_{ij} is the functional distance behavior for the interaction of i and j and was set as $\exp(-r)$. The region definition was set as molecular extents, and the ligand was selected as the molecule. All other parameters were set as the default values, as recommended in the HINT program.

2. Analysis by Site-Directed Mutagenesis. (a) Plasmid constructs and site-directed mutagenesis: The cDNA encoding the second cysteine-rich domain of PKCδ (C1b domain) was subcloned into the GST prokaryotic gene fusion vector pGEX-2TK as described previously.[41] Point mutations in the C1b domain were generated by using the Unique Site Elimination (U.S.E.) Mutagenesis Kit (Pharmacia Biotech., Piscataway, NJ). The sequences of the primers employed were as described,[41] and all mutations were confirmed by sequencing (Paragon, Baltimore, MD). The different plasmids for the mutated C1b domains were used to express the corresponding GST fusion proteins in *E. coli*.

(b) Ligand binding assay: The binding affinities of the isolated C1b domains of PKCδ were measured with [^{3}H]PDBu using the poly(ethylene glycol) precipitation method.[6] Briefly, purified GST fusion proteins or total lysates from *E. coli* expressing the GST fusion proteins (mutants and wild type) were incubated at 18 °C for 5 min in an assay mixture containing 100 μg/μL phosphatidylserine, 1 mM EGTA, [^{3}H]-PDBu, and, when appropriate, different concentrations of nonradioactive PDBu or (−)-ILV. Proteins were precipitated by addition of 35% poly(ethylene glycol), and after centrifugation, the radioactivity in the supernatant and the pellet was assessed. Because [^{3}H]PDBu and ligands were found for the various constructs to reequilibrate rapidly, final ligand concentrations were used in all calculations.

Results and Discussion

Computational Docking Studies. To test whether the MCDOCK program can correctly predict the experimentally determined binding mode, we first employed the MCDOCK program[29] to predict the binding mode for phorbol-13-acetate, whose experimental binding mode was previously determined by X-ray crystallography.[11] The X-ray structure of phorbol-13-acetate in complex with PKCδ C1b showed that the phorbol-13-acetate binds to PKC in a highly conserved hydrophobic region, formed by residues 8−12 and 20−27.[11] Therefore, the binding pocket formed by residues 8−12 and 20−27 was used as the binding site in the MCDOCK docking simulations, and the conformation of the binding site was taken from the X-ray structure of PKCδ C1b (CRD2) in complex with phorbol-13-acetate. The initial structure of phorbol-13-acetate for the MCDOCK docking simulations was obtained from the X-ray structure of phorbol-13-acetate in complex with PKCδ C1b, and hydrogen atoms were added using the QUANTA program.[31] The structure was then minimized using the CHARMM program. Phorbol-13-acetate contains a total of four rotatable bonds. To avoid bias, the four torsion angles associated with these four rotatable bonds were randomly sampled before MCDOCK docking simulations. During docking simulations, these four torsion angles were included in the sampling. Since the MCDOCK employs a Monte Carlo simulation technique, multiple docking simulations are necessary in order to obtain reliable results. A total of 100 MCDOCK simulations were performed with 1 000 000 MC steps for each simulation. Each simulation took about 15 min on an SGI Indigo2/R10000 computer.

The root-mean-square (rms) values between the 100 MCDOCK-predicted binding modes for phorbol-13-acetate and the X-ray determined structure were computed. In Figure 1, the interaction energies are plotted against the rms values for these 100 MCDOCK simulations. As can be seen, the binding modes predicted by these 100 MCDOCK runs roughly belong to three different clusters. The first cluster consists of more than 60 MCDOCK runs, and the rms values for the binding modes in this cluster are all less than or close to 2.0 Å. Within this cluster, the 40 MCDOCK runs with lowest interaction energy have rms values less than 1.7 Å. The five binding modes with the lowest interaction energies have rms values less than 0.5 Å, and the predicted

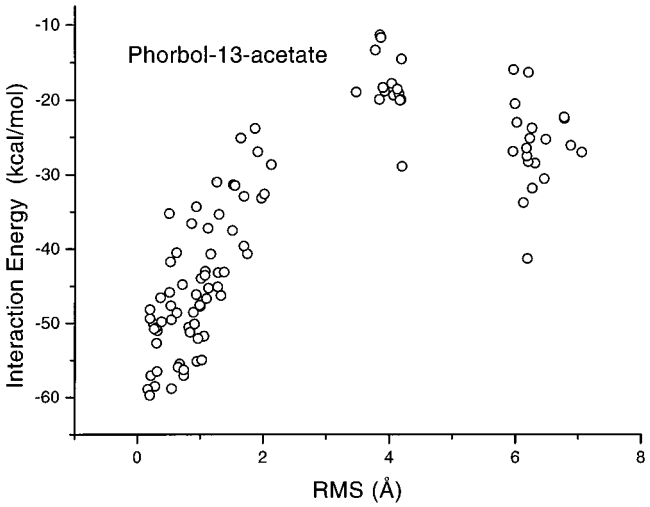

Figure 1. Interaction energy between the PKC C1b and phorbol-13-acetate obtained from each of the 100 MCDOCK simulations versus the rms of the calculated binding mode of phorbol-13-acetate from each MCDOCK simulation superimposed onto the X-ray-determined binding mode.

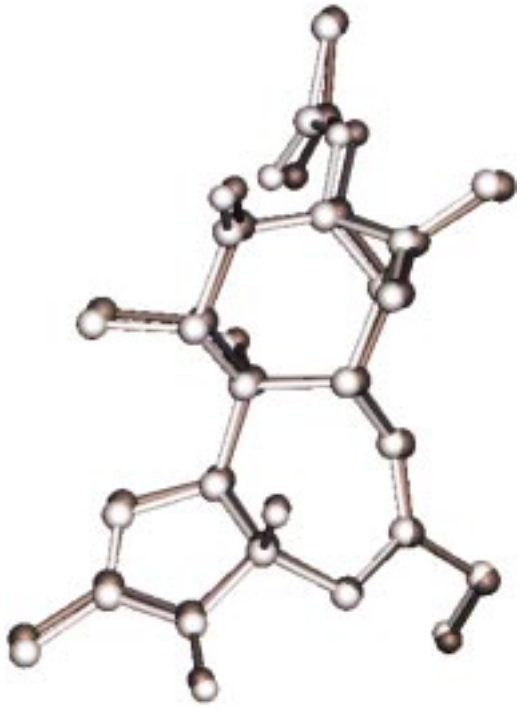

Figure 2. Superposition of the X-ray-determined binding mode of phorbol-13-acetate (dark color) and the MCDOCK-predicted binding mode with the lowest interaction energy among 100 MCDOCK simulations (light color).

binding mode with the lowest interaction energy is almost identical to the X-ray structure and has an rms value of 0.2 Å. The best binding mode predicted by the MCDOCK program and the experimentally determined binding mode from X-ray diffraction are shown in Figure 2. As can be seen, these two binding modes are almost indistinguishable. In addition to the binding modes very close to the X-ray structure, two very different binding modes were predicted with rms values of ca. 4 and 6 Å, respectively, as compared to the X-ray structure. However, the best binding modes within these two clusters have interaction energies 30 and 15 kcal/mol, respectively, higher than the best binding mode. These results

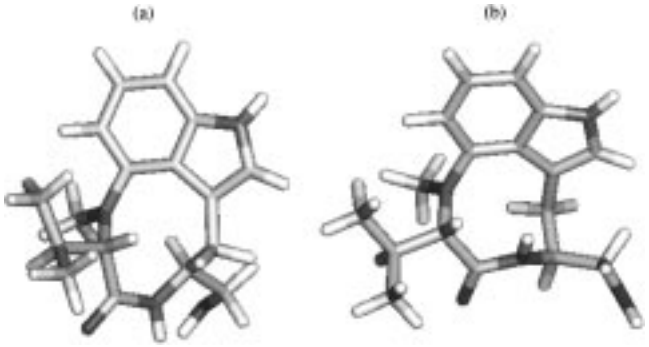

Figure 3. Two major conformations of ILV in solution: (a) cis-twist conformation and (b) trans-sofa conformation.

show that the MCDOCK can accurately predict the X-ray-determined binding mode for phorbol-13-acetate, taking into account the conformational flexibility of the ligand.

Experimentally, ILV and PDBu compete with each other for binding to PKC. Furthermore, our site-directed mutagenesis showed that the mutations of residues Pro 11 and Leu 20 to Gly and Gln 27 to Ala greatly reduce the binding affinities of both PDBu and ILV to these mutants.[28] These data strongly indicated that ILV and PDBu have a common binding site. Therefore, the binding pocket formed by residues 8−12 and 20−27 was selected as the potential binding site for ILV and used in the docking simulations.

ILV exists in two major conformations in solution, namely cis-twist and trans-sofa forms (Figure 3).[24] Recent experimental evidence[27,28] strongly suggested that the cis-twist conformation is most likely the active conformation of ILV, but the structural basis for such conformational preference was not entirely clear. To achieve a better understanding of the conformation preference of ILV, we have investigated the binding mode of both the cis-twist and trans-sofa conformations of ILV to PKC.

100 MCDOCK runs with 1 000 000 MC steps in each MCDOCK simulation were carried out on both the cis-twist and trans-sofa conformations of ILV. ILV has three rotatable bonds in its structure: one associated with the isopropyl group at C12 and two associated with the CH_2-OH group at C9. These two groups can adopt multiple low-energy conformations, and it is difficult to determine a priori its active binding conformation to PKC. For this reason, these three rotatable bonds were included in the sampling during MCDOCK docking simulations in order to obtain an accurate prediction.

Unlike the case of phorbol-13-acetate, the experimental binding mode for ILV is not known. To evaluate the simulation results, the binding mode with the lowest interaction energy (the best binding mode) obtained from the 100 MCDOCK simulations was identified. The rms values for ILV between the best binding mode and all other binding modes obtained from these MCDOCK runs were computed. In Figure 4, the interaction energies obtained for these 100 MCDOCK runs are plotted against the rms values. As can be seen, these 100 MCDOCK runs yield three different clusters based upon the rms values. Within each cluster, the predicted binding modes are either similar or identical. Thus, three possible binding modes were predicted.

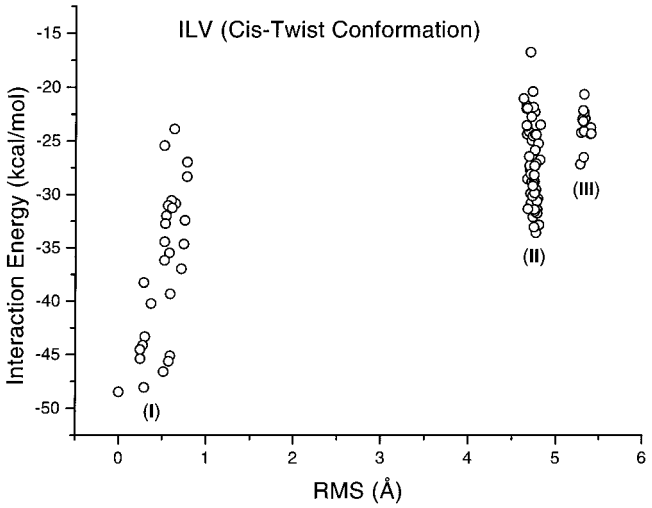

Figure 4. Interaction energy between the PKC C1b and ILV with its cis-twist conformation obtained from each of the 100 MCDOCK simulations versus the rms of the calculated binding mode of ILV from each MCDOCK simulation superimposed onto the predicted binding mode with the lowest interaction energy among the 100 MCDOCK simulations.

As evident from Figure 4, a number of complex structures in cluster I have interaction energies of more than 15 kcal/mol better than the best (lowest energy) complex structures in clusters II and III. Thus, the binding mode in cluster I most likely represents the "correct" binding mode for ILV if ILV adopts the cis-twist conformation. The binding mode with the lowest interaction energy was further minimized using the CHARMM program[33] and is depicted in Figure 5.

ILV equilibrates between the cis-twist and trans-sofa conformations in solution. Thus, the trans-sofa conformation is also a possible active conformation binding to PKC. To investigate this possibility, a total of 100 MCDOCK simulations were performed starting from the trans-sofa conformation of ILV. Identical simulation conditions were used as for the cis-twist conformation. Again, the binding mode with the lowest energy was identified and the rms values for all the atoms in ILV between all other binding modes, and the binding mode with lowest energy were computed. In Figure 6, the interaction energies obtained for these 100 MCDOCK simulations are plotted against the rms values.

As can be seen from Figure 6, the predicted binding modes for ILV in its trans-sofa conformation from these 100 MCDOCK runs are more scattered than those for ILV in its cis-twist conformation (Figure 4). The majority of these 100 MCDOCK runs can be roughly classified into two clusters. The lowest interaction energies within these two clusters are within 1 kcal/mol. It is of importance to note that the best binding mode for ILV in its trans-sofa conformation obtained from 100 MCDOCK runs has an interaction energy 15 kcal/mol less favorable than the best binding mode for ILV in its cis-twist conformation. Therefore, ILV most likely interacts with PKC in its cis-twist conformation with the binding mode shown in Figure 5.

Analysis of the Binding Mode of ILV in Its Twist Conformation. In the best binding model (lowest energy) derived for the cis-twist conformation of ILV (Figure 5), the ligand forms five hydrogen bonds with PKC. The primary hydroxyl group of ILV forms two hydrogen bonds: one with the amido group of Thr 12 and one with the carbonyl group of Leu 21 in PKC. This primary hydroxyl group of ILV is thus equivalent to the primary hydroxyl group of the phorbol esters. The carbonyl group at position 11 of ILV forms a hydrogen bond with the amido group of Gly 23, and the amido group at position 10 of ILV forms a hydrogen bond with the carbonyl group of Leu 21. Finally, the NH group at position 1 of ILV forms a weak hydrogen bond with the backbone carbonyl group of Met 9 (not shown in Figure 5).

To quantitatively assess these hydrogen bonds, we analyzed the crucial geometric parameters (Table 1). In

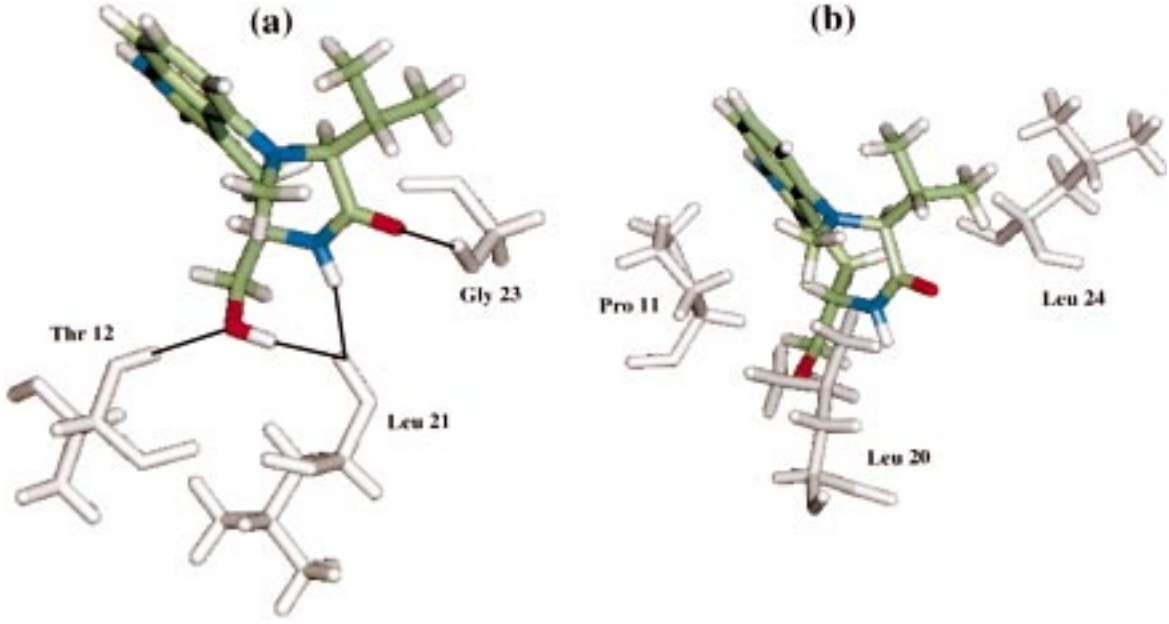

Figure 5. Predicted binding mode for ILV in its cis-twist conformation with the lowest interaction energy based upon the 100 MCDOCK simulations: (a) hydrogen bond network formed between ILV and the receptor; (b) hydrophobic contacts between ILV and the receptor.

Table 1. Hydrogen Bonds Formed between PKC and ILV in its Twist Conformation

donor	acceptor	r_{AD} (Å)	θ_{A-H-D} (deg)	θ_{AA-A-H} (deg)	E_{HB} (kcal/mol)	ratio (E_{HB}/E_{HB}optimal)
N−H (Thr 12, PKC)	O−H (14, ILV)	2.90	168.5	115.2	−3.77	0.94
O−H (14, ILV)	C=O (Leu 21, PKC)	2.72	152.1	134.4	−2.54	0.64
N−H (10, ILV)	C=O (Leu 21, PKC)	2.82	155.0	157.3	−2.47	0.62
N−H (Gly 23, PKC)	C=O (11, ILV)	2.91	164.4	123.5	−3.66	0.92
N−H (1, ILV)	C=O (Met 9, PKC)	2.81	127.2	110.9	−0.34	0.09
sum					−12.78	

Table 2. Hydrophobic Interaction Analysis Using the HINT Program on the PKC/ILV Twist Binding Model

atoms or groups in ILV	interacting with atoms or groups in PKC	HINT hydrophobic interaction score	% of total
isopropyl group at C12	Leu 20, Gly 23, Leu 24	75	16
N-methyl	Pro 11, Leu 20	187	39
indole ring	Tyr 8, Ser 10, Pro 11	67	14
C8	Tyr 8, Pro 11, Gly 23, Gln 27	22	4
C14	Tyr 8, Pro 11, Leu 20, Leu 21, Gln 27	62	13
C11	Leu 20, Trp 22, Gly 23, Gln 27	60	12
other atoms in ILV		9	2
residues in PKC	**interacting with atoms in ILV**	**HINT hydrophobic interaction score**	**% of total**
Tyr 8	C8, indole ring, C14	19	4
Ser 10	indole ring	2	<1
Pro 11	C8, indole ring, C14, *N*-methyl	130	27
Leu 20	C9, C11, C12, isopropyl group, *N*-methyl	194	40
Leu 21	C14	8	2
Trp 22	C11	5	1
Gly 23	C11, C8, isopropyl group	24	5
Leu 24	isopropyl group	64	13
Gln 27	C8, C9, C11, C14	36	7
total		482	100

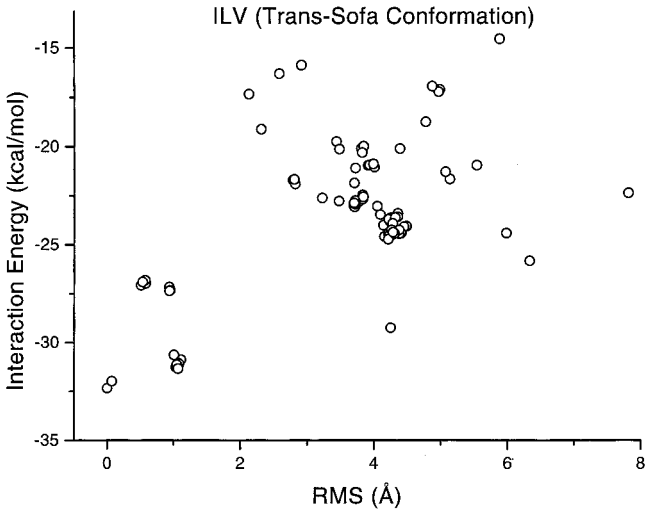

Figure 6. Interaction energy between the PKC C1b and ILV with its trans-sofa conformation obtained from each of the 100 MCDOCK simulations versus the rms of the calculated binding mode of ILV from each MCDOCK simulation superimposed onto the predicted binding mode with the lowest interaction energy among the 100 MCDOCK simulations.

addition, using eq 1 and assuming the optimal value of 4.0 kcal/mol for each hydrogen bond, we also estimated the hydrogen bond energy for each hydrogen bond and the ratio between hydrogen bond energy and its optimal value. These data are summarized in Table 1. It is clear that two of these five hydrogen bonds, formed between the amido group of Thr 12 and the primary hydroxyl group of ILV and between the amido group of Gly 23 and the carbonyl group of ILV, are nearly optimal. Two other hydrogen bonds, formed between the carbonyl group of Leu 21 and the primary hydroxyl group of ILV and between the carbonyl group of Leu 21 and the amido group of ILV, although less than optimal, are still fairly strong. One hydrogen bond, formed between the indole NH of ILV and the carbonyl group of Met 9, is weak, with an estimated hydrogen bond energy of only 0.34 kcal/mol. The total hydrogen bond energy in this binding model was estimated to be −12.78 kcal/mol.

In this binding model, a number of hydrophobic groups of ILV are in close proximity to several hydrophobic residues in PKC C1b. The isopropyl group at position 12 of ILV interacts well with the side chain of Leu 24. The *N*-methyl group at position 13 interacts with both the side chains of Leu 20 and Pro 11. The indole ring of ILV resides on the top of the wall formed by Met 9, Ser 10, and Pro 11 in PKC. Along with hydrogen bond formation, these hydrophobic interactions should contribute to the overall energetics of complex formation.

To gain a more quantitative understanding on these hydrophobic interactions, we have performed the HINT analysis[37−39] on the binding model for ILV. The results are summarized in Table 2. As can be seen, on the ligand side the HINT analysis clearly shows that the *N*-methyl group of ILV contributes the most to the hydrophobic interactions: 39% out of the total hydrophobic interaction scores. The isopropyl group at C12 of ILV contributes significantly. The indole ring of ILV contributes 14% to the total, suggesting its importance to the binding of ILV to PKC. It is of interest to note that three additional carbon atoms, C8, C11, and C14, make significant contributions to the overall hydrophobic interactions. On the receptor side, the two most important residues for the hydrophobic interactions are Pro 11 and Leu 20; together they account for 67% of the total scores. Leu 24 contributes 13% to the total. Gln 27 has a 7% contribution to the total hydrophobic interactions, primarily from its two carbon atoms on its

Table 3. Analysis by Site-Directed Mutagenesis of the Binding of ILV and PDBu to PKC C1b

	ILV		PDBu	
	K_i (nM)	ratio (mutant/wild-type)	K_i (nM)	ratio (mutant/wild-type)
wild-type	2.01 ± 0.17		0.351 ± 0.054	
mutant (Tyr8 → Gly)	658 ± 29	327	18.4 ± 1.4	52.4
mutant (Pro 11 → Gly)	7080 ± 770	3520	210 ± 15	598
mutant (Thr 12 → Gly)	25.3 ± 2.5	12.6	1.24 ± 0.23	3.53
mutant (Phe 13 → Gly)	10.9 ± 0.8	5.4	0.82 ± 0.13	2.33
mutant (Leu 20 → Gly)	66.2 ± 6.2	32.9	6.59 ± 0.3	15
mutant (Leu 21 → Gly)	nd[a]		no binding	>1000
mutant (Trp 22 → Gly)	nd		25.0	31.2
mutant (Leu 24 → Gly)	nd		no binding	>1000
mutant (Gln 27 → Gly)	nd		no binding	>1000
mutant (Gln 27 → Val)	1100 ± 140	552	14.2 ± 1.5	40.4
mutant (Gln 27 → Trp)	nd		no binding	>1000

[a] nd, not determined. If the mutant does not have a significant binding to the reference ligand, PDBu, the binding affinity of the mutant to ILV cannot be determined.

side chain. The remaining residues in the binding site, including Tyr 8, Ser 10, Leu 21, Trp 22, and Gly 23, each contributes not greater than 5% to the total hydrophobic scores.

Previously, we have reported the molecular modeling studies of benzolactam binding to PKCδ C1b.[28] Benzolactam, which was designed based upon ILV, has a binding affinity 30-fold weaker than that of ILV. A comparison of the binding models of ILV and benzolactam shows that they bind in a similar binding manner, including an identical hydrogen-bonding network between the ligands and the receptor and similar hydrophobic interactions. The crucial difference between these two ligands is that the hydrophobic contact between Pro 11 and ILV is missing in the binding mode for benzolactam, which may explain in part the weaker binding affinity of benzolactam. Recently, a computational docking simulation was performed by Endo et al. on teleocidin and benzolactam analogues using an automatic docking program (ADAM).[30] Their results are in good agreement with our previously published results for benzolactam obtained by molecular modeling and our current results for ILV obtained using the MCDOCK simulations. Taken together, these different computational studies predict binding models for teleocidin, ILV, and their analogues that are consistent with each other, suggesting that the predicted binding modes for these ligands are likely to be the "correct" binding modes.

Structure−Activity Relationships (SARs). It is important to validate our predicted binding mode with the SARs of ILV and its analogues. Previous efforts have accumulated a large body of SARs for this class of PKC ligands.[27,28,30,42−52] The SARs for this class of compounds clearly indicate that the trans-sofa conformation of ILV is unlikely to be the active conformation and the cis-twist conformation is the biologically active one.[25−27,50] All analogues that exclusively adopt the trans-sofa conformation are totally inactive.[25−27,50] This is entirely consistent with our docking results, which show that ILV in its cis-twist conformation can orient in such a way so as to facilitate the maximum hydrophilic and hydrophobic interactions with PKC. The *cis*-amide bond makes it possible for the amide group to form three strong hydrogen bonds with the receptor. The importance of the primary hydroxyl group and its stereochemistry in ILV and its analogues is reflected by the two strong hydrogen bonds formed between this group and PKC. ILV analogues either with incorrect stereochemistry at this position or without the hydroxyl group are poorly active or inactive.[43,48,49] The minimal significance of the NH group at position 1 of ILV and its analogues can be seen from the relatively small decrease in activity shown by the benzofuran analogue of ILV,[52] as compared to ILV. This is in agreement with the weak hydrogen bond formed between this group of ILV and the carbonyl group of Met 9 in PKC in the best binding mode for ILV (Figure 5).

Our studies shed light on the importance of the "specific" hydrophobic−hydrophobic interactions between ILV and PKC. On the basis of our results, the importance of the isopropyl group is primarily due to the interactions between this group and Leu 24. Indeed, indolactam-G, which lacks the isopropyl group, is 74-fold less potent than ILV,[48] and indolactam-A, in which the isopropyl group is replaced by a methyl group, is 7-fold less potent than ILV.[48] A slightly larger hydrophobic group in this position can improve the hydrophobic−hydrophobic interactions, and this can seen from the 5-fold increase of the activity for indolactam-TL, as compared to ILV.[48] The *N*-methyl group was found to have strong hydrophobic−hydrophobic interactions. Indeed, an analogue which lacks this methyl group was found to be at least 100-fold less potent than ILV.[50] Although the NH group in the indole ring only forms a weak hydrogen bond with the receptor, the indole ring itself was shown to be important for the hydrophobic interactions. Thus, the benzolactam-V-8 without a long hydrophobic tail, which adopts the desired conformation but has less hydrophobic interactions at this site, is 30-fold less potent than ILV.[28]

Analysis by Site-Directed Mutagenesis. Our previous mutagenesis studies have revealed a number of residues in PKCδ C1b that are important to the binding of phorbol ester to PKC.[41] Under the same assay conditions as for ILV, the binding affinities of PDBu for each mutant are summarized in Table 3. Consistent with the X-ray structure,[11] the mutational analysis showed the important roles played by residues Pro 11, Leu 20, Leu 21, Leu 24, and Gln 27.[41] These residues are conserved among PKC isozymes and were shown to be directly involved in the interactions between phorbol ester and PKC in the X-ray structure.[11] Whereas the mutations of Pro 11 and Leu 20 to Gly quantitatively reduce the binding affinity of PDBu to the receptor, the mutations of Leu 21, Leu 24, and Gln 27 to Gly abolish any measurable binding.[32]

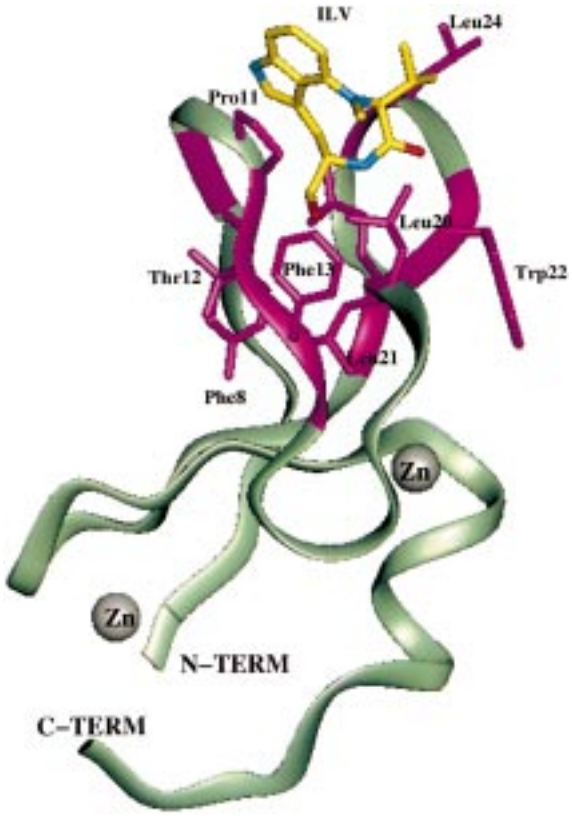

Figure 7. ILV in complex with PKC C1b. ILV is shown in yellow, and the residues that have been mutated in PKC C1b are colored purple. Oxygen and nitrogen atoms are shown in red and blue, respectively, in the side chains of these mutated residues and in ILV.

To quantitatively assess the contributions of these crucial residues to the binding of ILV to PKCδ C1b and to provide further validation of the predicted binding model for ILV obtained using the computational docking approach, we have determined the effects of single mutations on nine crucial residues around the binding site, including Tyr 8, Pro 11, Thr 12, Phe 13, Leu 20, Leu 21, Leu 24, and Gln 27 (Figure 7). Except for Gln 27, the residues were mutated to Gly. For Gln 27, it was mutated either to Gly or to Val or to Trp. Mutations of Leu 21 to Gly, Leu 24 to Gly, Gln 27 to Gly, and Gln 27 to Trp all result in a mutant with no measurable binding affinity to PDBu, the reference ligand. Thus, the binding affinity of these mutants to ILV could not be measured. For the other six mutants, the quantitative binding affinity of ILV to these mutants was measured and is provided in Table 3.

From Table 3, it is of note that for every single mutation in the binding site, the binding affinity for ILV is reduced more than that for PDBu. This may reflect the fact that ILV interacts with PKC through optimal hydrophobic and hydrogen bond interactions and PDBu appears to have optimal hydrogen bond interactions but less than optimal hydrophobic interactions based upon our modeling analysis and the X-ray structure.[11] The mutation of Pro 11 to Gly reduces the binding affinity of both PDBu and ILV to PKC. For PDBu, the binding affinity is reduced by 600-fold, and for ILV, the binding affinity is reduced by 3500-fold. We have shown in our predicted binding model for ILV that Pro 11 plays an important role in the hydrophobic interactions with the indole ring and the *N*-methyl group in ILV. It is also known that proline residues in general are important for controlling protein conformation. Therefore, the 3500-fold decrease in the binding affinity may reflect both the loss of some hydrophobic interactions at this site and the effect of the conformational change in the binding site. It is, however, difficult to separate these two factors.

The mutation of Thr 12 to Gly has a significant impact on the binding of ILV to PKC, while it has less effect on the binding of PDBu to PKC. This mutation reduces the binding of ILV and of PDBU to the receptor by 12.6- and 3.5-fold, respectively. In our predicted binding model for ILV and the X-ray structure for phorbol-13-acetate, Thr 12 plays an important role in the binding by forming a strong hydrogen bond with the primary hydroxyl group in both ligands. Its side chain, however, was not involved in direct contact with the ligands. Therefore, the loss in binding affinity for ILV to the receptor in this case may mainly reflect the conformational change of the binding site upon mutation. The data for this mutant also clearly showed that ILV is more sensitive than PBDu to the conformational change in the binding site.

The results for the Phe 13 to Gly mutation are somewhat surprising. Both the X-ray structure and our modeling studies showed that this residue makes no direct contribution to the binding of PDBU and ILV to PKC. However, the binding of PDBu and ILV to this mutant is reduced by 2.3- and 5.4-fold, respectively. A possible explanation is that this mutation may have affected the conformation of Thr 12, which in turn affected the binding of PDBU and ILV to the receptor.

The mutation of Leu 20 to Gly reduces the binding affinity to the receptor by 32.9-fold for ILV and 18.7-fold for PDBu, respectively. In our predicted binding model for ILV, this residue has strong hydrophobic−hydrophobic interactions with ILV, primarily with the *N*-methyl group and part of the indole ring. The X-ray structure showed that the hydrophobic side chain of Leu 20 does not participate in the internal folding of the protein; thus the side chain of this residue is not important to the conformation in the binding site. As a consequence, the reduction in the binding affinity for ILV and PDBu may solely reflect the loss in the hydrophobic−hydrophobic interactions between the receptor and the ligands at this site.

Leu 24 was shown to be involved in the hydrophobic−hydrophobic interactions with ILV. The mutation of Leu 24 to Gly completely abolishes the binding of PDBu to the receptor.[32] Since PDBu was used as the reference ligand, we were therefore unable to measure the binding affinity of ILV to this mutant. Our modeling analysis shows that Leu 24 plays an important role in the binding of ILV to PKC through hydrophobic−hydrophobic interactions. On the basis of the X-ray structure of phorbol-13-acetate in complex with PKCδ C1b, the hydrophobic side chain of Leu 24 is in close proximity with the hydrophobic moieties in the phorbol ester, suggesting hydrophobic interactions. The complete loss of the binding of PDBu to this mutant is therefore in part due to the decrease in the hydrophobic interactions. It should also be pointed out that the mutation of Leu 24 to Gly places two Gly residues adjacent in the mutant

(Gly 23 and Gly 24), and this may have a profound impact on the conformation of Gly 23. Since Gly 23 has been shown to form strong hydrogen bond(s) with phorbol ester and ILV, the complete loss in the binding of PDBu to PKC may also reflect the consequence of the conformational change caused by the mutation.

Gln 27 plays a key role in the conformation of the binding site through formation of two hydrogen bonds with Tyr 8 and one hydrogen bond with Gly 23.[11] The mutation of Gln 27 to Gly completely abolishes the binding of PDBu to PKC, suggesting significant conformational changes may have occurred in the binding site with this mutation.[32] The mutation of Gln 27 to Val reduces the binding affinity of both ILV and PDBu to the receptor by 552- and 40.4-fold, respectively. However, it is clear that significant binding to both ILV and PDBu is retained by this mutant. This suggests that although Val cannot fully restore the desired conformation in the binding site, the conformational change caused by this mutation is small enough to allow some binding of both ILV and PDBu to the receptor. It is noted, however, that the mutation of Glu 27 to Val reduces the binding affinity for ILV by more than 500-fold and only 40.4-fold for PDBu, indicating again that ILV is more sensitive to the conformational change in the binding site than PDBu.

Previously, we have determined the binding affinities of three mutants (Pro 11 → Gly, Leu 20 → Gly, Gln 27 → Val) to benzolactam, an analogue of ILV.[28] As compared to ILV, benzolactam experiences consistent reduction in binding affinity in these three mutants. However, in each case, the binding affinity of ILV to these mutants is reduced more dramatically than that of benzolactam. While the mutation of Pro 11 to Gly reduces the binding affinity of benzolactam by 68-fold, it reduces the binding affinity of ILV by 3520-fold. This is entirely consistent with our predicted binding models for ILV and benzolactam. In our predicted binding models, while ILV and benzolactam interact with PKC in a similar manner, ILV has a larger interaction surface with PKC than benzolactam. This is due to the fact that ILV interacts with Pro 11 through its indole ring with a relatively larger surface area, while benzolactam interacts with Pro 11 through its benzo group with a relatively smaller surface area. The mutation of Leu 20 to Gly reduces the binding affinity of benzolactam by 13-fold, while it reduces the binding affinity of ILV by 32.9-fold. The mutation of Gln 27 to Val reduces the binding affinity of benzolactam by 88-fold, while it reduces the binding affinity of ILV by 552-fold. However, on the basis of our predicted binding models for ILV and benzolactam, these two ligands have identical interaction manners with Leu 20 and Gln 27. Thus, our mutation data, together with our molecular modeling studies, indicate that even if two ligands bind to their receptor in a similar manner, the ligand with the higher binding affinity will be more sensitive to the perturbation made to the binding site of the receptor.

In summary, our analysis by site-directed mutagenesis confirmed our predicted binding model for ILV and provided quantitative assessments on the contributions of a number of crucial residues to the binding of ILV and PDBu to PKC. This information provides important insight into the structural basis of PKC ligands binding to PKC and may be valuable for the design of new PKC ligands.

Pharmacophores for ILV and Phorbol Esters. On the basis of our docking studies, the interactions between ILV and PKC constitute of a number of strong hydrogen bonds and several specific hydrophobic−hydrophobic interactions. Two strong hydrogen bonds are formed between the primary hydroxyl group of ILV and the carbonyl group of Leu 21 and the amido group of Thr 12. One strong hydrogen bond is formed between the carbonyl group of ILV and the amido group of Gly 23. Another strong hydrogen bond is formed between the amido group of ILV and the carbonyl group of Leu 21. It was found that the NH group at position 1 of ILV only forms a fairly weak hydrogen bond with the carbonyl group of Met 9. The X-ray structure of phorbol-13-acetate in complex with PKCδ C1b shows that phorbol-13-acetate also forms four strong hydrogen bonds with the receptor.[11] Three out of these four hydrogen bonds formed between phorbol-13-acetate and PKC are found in the binding models for ILV. It should be noted that for each class of PKC ligands, one unique hydrogen bond is found. In the case of phorbol-13-acetate, the unique, strong hydrogen bond was formed between the hydroxyl group at the C4 position with the carbonyl group of Gly 23. In the case of ILV, the unique hydrogen bond is formed between the amido group in ILV and the carbonyl group of Leu 21. The strong, common hydrogen bonds shared between phorbol esters and ILV explain why these ligands compete with each other for binding to PKC, as shown experimentally. The unique hydrogen bonds formed for ILV and phorbol-13-acetate also demonstrate that although these ligands occupy a common binding site in PKC, each class of ligands is recognized by the receptor through the combination of common and unique hydrogen bonds. Therefore, if one views the PKC ligand "pharmacophore" as comprising a set of common hydrogen bond-donating/accepting atoms/groups, these two classes of ligands do not share a common 3D pharmacophore. Or alternatively, one can perceive that these ligands do share a common 3D "receptor" pharmacophore, but not a common 3D "ligand" pharmacophore. This distinction may be useful and important in the development of novel PKC ligands with distinct binding features. Our finding that even high-affinity ligands (ILV and phorbol esters) binding to a common receptor binding site (PKC) may have different "pharmacophores" should have general implications for pharmacophore mapping and identification based upon the structures of ligands, as well as for rational drug design.

Summary and Conclusions

Computational docking simulations and site-directed mutagenesis were performed to probe the binding of ILV to PKC. Unlike our previous molecular modeling study, the present study employed an automated docking program, MCDOCK, to predict the binding mode of ILV to PKC to eliminate the possible bias introduced in the molecular modeling studies. Through docking simulations, we have determined the cis-twist conformation of ILV to be the active conformation binding to PKC and have identified the precise 3D structure of ILV in

complex with PKC C1b. Through the quantitative analysis of the hydrogen bond and hydrophobic interactions between ILV and PKC, a clear understanding of the interactions between ILV and PKC was achieved. This binding model was validated by the SARs of ILV and its analogues and was found to be entirely consistent with all known SAR data. Site-directed mutagenesis was performed on a number of crucial residues in the binding site of PKC, and quantitative binding affinities of these mutants to ILV and PDBu were determined. Our site-direct mutagenesis provides a quantitative assessment of the contributions of these conserved residues to the binding of ILV and PDBU to PKC. These studies provide important insights into the interactions between PKC ligands and PKC, and this information may prove to be invaluable to the design of new PKC ligands. One of our long-term goals is to design potent, structurally simple, isozyme-selective PKC ligands. With the knowledge gained from the current studies, we are poised for such a task. Indeed, on the basis of the predicted binding mode for ILV, a novel class of PKC ligands, certain substituted pyrrolidones, were designed[53] to capture the crucial hydrogen bonds and to maximize the hydrophobic interactions as observed for ILV in its predicted binding mode (Figure 5). Thus far, this new class of PKC ligands has achieved nanomolar potency.[53] We believe that our successful design of structurally novel and potent PKC ligands further validates our predicted binding model of ILV.

References

(1) Nishizuka, Y. The role of protein kinase C in cell surface signal transduction and tumor promotion. *Nature* **1984**, *308*, 693−698.

(2) Nishizuka, Y. Studies and perspectives of protein kinase C. *Science* **1986**, *233*, 305−312.

(3) Nishizuka, Y. The molecular heterogeneity of protein kinase C and its implications for cellular recognition. *Nature* **1988**, *334*, 661−65.

(4) Lester, D. S., Epand, R. M., Eds.; *Protein kinase C, current concepts and future perspectives*; Ellis Horword Ltd.: New York, 1992.

(5) Kazanietz, M. G.; Areces, L. B.; Bahador, A.; Mischak, H.; Goodnight, J.; Mushinski, F.; Blumberg, P. M. Characterization of ligand and substrate specificity for the calcium-dependent and calcium-independent PKC isozymes. *Mol. Pharmacol*. **1993**, *44*, 298−307.

(6) Sharkey, N. A.; Blumberg, P. M. Comparison of the activity of phorbol 12-myristate 13-acetate and the diglyceride glycerol 1-myristate 2-acetate. *Carcinogenesis* **1986**, *7*, 677−679.

(7) Blumberg, P. M. Protein kinase C as the receptor for the phorbol ester tumor promoters. Sixth Rhoads Memorial Award Lecture. *Cancer Res*. **1988**, *48*, 1−8.

(8) Burns, D. J.; Bell, R. M. Protein kinase C contains two phorbol ester binding domains. *J. Biol. Chem*. **1991**, *266*, 18330−18338.

(9) Quest, A. F. G.; Bardes, E. S. G.; Bell, R. M. A phorbol ester binding domain of protein kinase C gamma. High affinity binding to a glutathione-S-transferase/Cys2 fusion protein. *J. Biol. Chem*. **1994**, *269*, 2953−2960.

(10) Kazanietz, M. G.; Lewin, N. E.; Gao, F.; Pettit, G. R.; Blumberg, P. M. Binding of [26-^{3}H]bryostatin 1 and analogues to calcium-dependent and calcium-independent PKC isozymes. *Mol. Pharmacol*. **1994**, *46*, 374−379.

(11) Zhang, G.; Kazanietz, M. G.; Blumberg, P. M.; Hurley, J. H. Crystal structure of the cys2 activator-binding domain of protein kinase C in complex with phorbol ester. *Cell* **1995**, *81*, 917−924.

(12) Jeffrey, A. M.; Liskamp, R. M. J. Computer-assisted molecular modeling of tumor promoters: Rationale for the activity of phorbol esters, teleocidin B and aplysiatoxin. *Proc. Natl. Acad. Sci. U.S.A*. **1986**, *83*, 241−245.

(13) Wender, P. A.; Koehler, K. G.; Sharkey, N. A.; Dell'Aquila, M. L.; Blumberg, P. M. Analysis of the phorbol ester pharmacophore on protein kinase C as a guide to the rational design of new classes of analogues. *Proc. Natl. Acad. Sci. U.S.A*. **1986**, *83*, 4214−4218.

(14) Itai, A.; Kato, Y.; Tomioka, N.; Endo, Y.; Hasegawa, M.; Shudo, K.; Fujiki, H.; Sakai, S. A receptor model for tumor promoters: Rational superposition of teleocidins and phorbol esters. *Proc. Natl. Acad. Sci. U.S.A*. **1988**, *85*, 23688−23692.

(15) Wender, P. A.; Cribbs, C. M.; Koehler, K. G.; Sharkey, N. A.; Herald, C. L.; Kamano, Y.; Pettit, G. R.; Blumberg, P. M. Modeling of the bryostatins to the phorbol ester pharmacophore on protein kinase C.. *Proc. Natl. Acad. Sci. U.S.A*. **1988**, *85*, 7197−7201.

(16) Nakamura, H.; Kishi, Y.; Pajares, M. A.; Rando, R. R. Structural basis of protein kinase C activation by tumor promoters. *Proc. Natl. Acad. Sci. U.S.A*. **1989**, *86*, 9672−9676.

(17) Kong, F.; Kishi, Y.; Perez-Sala, D.; Rando, R. R. The pharmacophore of debromoaplysiatoxin responsible for protein kinase C activation. *Proc. Natl. Acad. Sci. U.S.A*. **1991**, *88*, 1973−1976.

(18) Rando, R.; Kishi, Y. Structural basis of protein kinase C activation by diacylglycerols and tumor promoters. *Biochemistry* **1992**, *31*, 2211−2218.

(19) Sharma, R.; Lee, J.; Wang, S.; Milne, G. W. A.; Lewin, N. E.; Blumberg, P. M.; Marquez, V. E. Conformationally constrained analogues of diacylglycerol. Ultrapotent protein kinase C (PK−C) ligands based on a racemic 5-(disubstituted tetrahydro-2-furanone. *J. Med. Chem*. **1996**, *39*, 19−28.

(20) Lee, J.; Wang, S.; Milne, G. W. A.; Sharma, R.; Lewin, N. E.; Blumberg, P. M.; Marquez, V. E. Conformationally constrained analogues of diacylglycerol. Ultrapotent protein kinase C (PK−C) ligands based on a chiral 5-(acyloxymethyl)-5-(hydroxymethyl)tetrahydro-2-furanone template. *J. Med. Chem*. **1996**, *39*, 29−35.

(21) Lee, J.; Sharma, R.; Wang, S.; Milne, G. W. A.; Lewin, N. E.; Blumberg, P. M.; Marquez, V. E. Conformationally constrained analogues of diacylglycerol. Ultrapotent protein kinase C (PK−C) ligands based on a chiral 4-disubstituted heptono-1,4-lactone template. *J. Med. Chem*. **1996**, *39*, 36−45.

(22) Wender, P. A.; DeBrabander, J.; Harran, P. G.; Jimerez, J.-M.; Koehler, M. F. T.; Lippa, B.; Park, C.-M.; Siedenbiedel, C.; Pettit, G. R. The Design, computer modeling, solution structure, and biological evaluation of synthetic analogues of bryostatin 1. *Proc. Natl. Acad. Sci. U.S.A*. **1998**, *95*, 6624−6629.

(23) Wang, S.; Zaharevitz, D.; Milne, G. W. A.; Sharma, R.; Marquez, V. E.; Lewin, N. E.; Blumberg, P. M. The discovery of novel, structurally diverse PK−C agonists through computer 3D-database pharmacophore search. Molecular modeling studies. *J. Med. Chem*. **1994**, *37*, 4479−4489.

(24) Endo, Y.; Hasegawa, M.; Itai, A.; Shudo, K.; Tori, M.; Asakawa, Y.; Sakai, S. Tumor promoters in two conformational states in solution. Stereochemistry of (±)-indolactam-V. *Tetrahedron Lett*. **1985**, *26*, 1069−1072.

(25) Kozikowski, A. P.; Ma, D.; Pang, Y.-P.; Shum, P.; Likic, V.; Mishra, P. K.; Macura, S.; Basu, A.; Lazo, J. S.; Ball, R. G. Synthesis, molecular modeling, 2-D-NMR, and biological evaluation of ILV mimics as potential modulators of protein kinase C. *J. Am. Chem. Soc*. **1993**, *115*, 3957−3965.

(26) Endo, Y.; Ohno, M.; Hirano, M.; Itai, A.; Shudo, K. Synthesis, conformation, and biological activity of teleocidin mimics, benzolactams. A clarification of the conformational flexibility problem in structure−activity studies of teleocidins. *J. Am. Chem. Soc*. **1996**, *118*, 1841−1855.

(27) Irie, K.; Isaka, T.; Iwata, Y.; Yanai, Y.; Nakamura, Y.; Koizumi, F.; Ohigashi, H.; Wender, P.; Satomi, Y.; Nishino. Synthesis and biological activities of new conformationally restricted analogues of (−)-indolactam-V: Elucidation of the biologically active conformation of the tumor-promoting teleocidins. *J. Am. Chem. Soc*. **1996**, *118*, 10733−10743.

(28) Kozikowski, A. P.; Wang, S.; Ma, D.; Yao, J.; Ahmad, S.; Glazer, R. I.; Bogi, K.; Acs, P.; Modarres, S.; Blumberg, P. M. Modeling, chemistry, and biology of the benzolactam analogues of ILV. 2. Identification of the binding site of the benzolactams in the CRD2 activator-binding domain of PKCδ and discovery of an ILV analogue of improved isozyme selectivity. *J. Med. Chem*. **1997**, *40*, 1316−1326.

(29) Liu, M.; Wang, S. MCDOCK: A Monte Carlo simulation approach to the molecular docking problem. *J. Comput.-Aided Mol. Des*. **1999**, *13*, 435−451.

(30) Harada, H.; Sakabe, N.; Hirata, Y.; Tomiie, Y.; Nitta, I. The X-ray structure determination of Dihydroteleocidin B monobromoacetate. *Bull. Chem. Soc. Jpn*. **1966**, *39*, 1773−1775. The X-ray corrdinates can be found in the Cambridge Structural Database under the code name TLOBDH10.

(31) QUANTA, a molecular modeling system, is supplied by Molecular Simulations Inc., 200 Fifth Ave, Waltham, MA 01803-5279.

(32) Frisch, M. J.; Truck, G. W.; Schlegel, H. B.; Robb, M. A.; Head-Gordon, M.; Replogle, E. S.; Gomperts, C.; Martin, R. L.; Fox, D. J.; Defrees, D. J.; Baker, J.; Stewart, J. J. P.; Pople, J. A. Gaussian 92/DFT, Revision G.4; Gaussian, Inc.: Pittsburgh, PA, 1993.

(33) Brooks, B. R.; Bruccoleri, R. E.; Olafson, B. D.; States, D. J.; Swaminathan, S.; Karplus, M. CHARMM: A program for macromolecular energy, minimization, and dynamics calculations. *J. Comput. Chem.* **1983**, *4*, 187−217.
(34) Jorgensen, W. L.; Chandrasekhar, J.; Madura, J. D.; Impey, R. W.; Klein, M. L. Comparison of simple potential functions for simulating liquid water. *J. Chem. Phys.* **1983**, *79*, 926−935.
(35) van Gunsteren, W. F.; Berendsen, H. J. C. Algorithms for macromolecular dynamics and constraint dynamics. *Mol. Phys.* **1977**, *34*, 1311−1327.
(36) Endo, Y.; Takehana, S.; Ohno, M.; Driedger, P. E.; Stabel, S.; Mizutani, M. Y.; Tomioka, N.; Itai, A.; Shudo, K. Clarification of the binding mode of teleocidin and benzolactams to the Cys2 domain of protein kinase Cδ by synthesis of hydrophobically modified, teleocidin-mimicking benzolactams and computational docking simulation. *J. Med. Chem.* **1998**, *41*, 1476−1496.
(37) The HINT program is supplied by eduSoft, LC, P.O. Box 1811, Ashland, VA 23005.
(38) Kellogg, G. E.; Joshi, G. S.; Abraham, D. J. New Tools for modeling and understanding hydrophobicity and hydrophobic interactions. *Med. Chem. Res.* **1992**, *1*, 444−453.
(39) Meng, E. C.; Kuntz, I. D.; Abraham, D. J.; Kellogg, G. E. Evaluating docked complexes with the HINT exponential function and empirical atomic hydrophobicities. *J. Comput.-Aided Mol. Des.* **1994**, *8*, 299−306.
(40) Chem-X is a product of Chemical Design Ltd., Roundway House, Cromwell Park, Chipping Norton, Oxon OX7 5SR, U.K.
(41) Kazanietz, M. G.; Wang, S.; Milne, G. W. A.; Lewin, N. E.; Liu, H. L.; Blumberg, P. M. Residues in the second cysteine-rich region of PKC relevant to phorbol ester binding as revealed by site-directed mutagenesis. *J. Biol. Chem.* **1995**, *270*, 21852−21859.
(42) Endo, Y.; Shudo, K.; Itai, A.; Hasegawa, M.; Sakai, S. Synthesis and stereochemistry of indolactam-V, An active fragment of teleocidins. Structural requirements for tumor-promoting activity. *Tetrahedron* **1986**, *42*, 5905−5924.
(43) Irie, K.; Koshimizu, K. Structure−activity studies of indole alkaloid tumor promoters. *Mem. Coll. Agric. Kyoto Univ.* **1988**, *132*, 1−59.
(44) Cardellina II, J. H.; Marner, F.; Moore, R. E.; Seaweed Dermatitis: Structure of lyngbyatoxin A. *Science* **1979**, *204*, 193−195.
(45) Hitotsuyanagi, Y.; Yamaguchi, K.; Ogata, K.; Aimi, N.; Sakai, S.; Koyama, Y.; Endo, Y.; Shudo, K.; Itai, A.; Iitaka, Y. Elucidation of the structures of olivoretin B and C. *Chem. Pharm. Bull.* **1984**, *32*, 3774−3778.
(46) Sakai, S.; Aimi, N.; Yamaguchi, K.; Hitotsuyanagi, Y.; Watanabe, C.; Yokose, K.; Koyama, Y.; Shudo, K.; Itai, A. Elucidation of the structure of olivoretin A and D (teleocidin B). *Chem. Pharm. Bull.* **1984**, *32*, 354−357.
(47) Kawai, T.; Ichinose, T.; Endo, Y.; Shudo, K.; Itai, A. Active conformation of a tumor promoter, teleocidin. A molecular dynamics study. *J. Med. Chem.* **1992**, *35*, 2248−2253.
(48) Fujiki, H.; Suganuma, M.; Nakayasu, M.; Endo, Y.; Shudo, K.; Sugimura, T. Structure−activity studies on synthetic analogues (indolactams) of the tumor promoter teleocidin. *Gann* **1984**, *75*, 866−870.
(49) Fujiki, H.; Suganuma, M.; Nakayasu, M.; Hakii, H.; Nakayasu, M.; Endo, Y.; Shudo, K.; Irie, K.; Koshimizu, K.; Sugimura, T. Tumor promoting activities of new synthetic analogues of teleocidin. *Proc. Jpn. Acad.* **1985**, *61*, 45−47.
(50) Irie, K.; Koshimizu, K. The indole alkaloid tumor promoter teleocidins as Epstein−Barr virus inducers: structure, biosynthesis and structure−activity relationship. In *Natural Products as Antiviral Agents*; Chu, C. K., Cutler, H. G., Eds.; Plenum Press: New York, 1992; pp 257−273.
(51) Endo, Y.; Imada, T.; Yamaguchi, K.; Shudo, K. Conformational states of indolactams: Structures of 13-*N*-desmethylindolactam-V and 13-*O*-indolactam-V. *Heterocycles* **1994**, *39*, 571−579.
(52) Kozikowski, A. P.; Ma, D.; Du, L.; Lewin, N. E.; Blumberg, P. M. Synthesis of the benzofuran analogue of ILV, a new protein kinase C (PKC) activator. *Bioorg. Med. Chem. Lett.* **1994**, *4*, 637−640.
(53) Qiao, L.; Wang, S.; George, C.; Lewin, N. E.; Blumberg, P. M.; Kozikowski, A. Structure-based design of a new class of protein kinase C modulators. *J. Am. Chem. Soc.* **1998**, *120*, 6629−6630.

JM990129N